INSTITUTE OF PHYSICS PUBLISHING COMBUSTION THEORY AND MODELLING

Combust. Theory Modelling **7** (2003) 317–332 PII: S1364-7830(03)38343-3

Flamelet modelling of non-premixed turbulent combustion with local extinction and re-ignition

Heinz Pitsch[1,3], **Chong M Cha**[1] **and Sergei Fedotov**[2]

[1] Center for Turbulence Research, Stanford University, Stanford, CA 94305-3030, USA
[2] Department of Mathematics, UMIST, Manchester, M60 1QD, UK

E-mail: H.Pitsch@stanford.edu, chongcha@aerodyne and Sergei.Fedotov@umist.ac.uk

Received 18 June 2002, in final form 5 March 2003
Published 3 April 2003
Online at stacks.iop.org/CTM/7/317

Abstract

Extinction and re-ignition in non-premixed turbulent combustion is investigated. A flamelet formulation accounting for transport along mixture fraction iso-surfaces is developed. A new transport term appears in the flamelet equations, which is modelled by a stochastic mixing approach. The timescale appearing in this model is obtained from the assumption that transport at constant mixture fraction is only caused by changes of the local scalar dissipation rate. The space coordinates appearing in this term can then be replaced by the mixture fraction and the scalar dissipation rate. The dissipation rate of the scalar dissipation rate appears as a diffusion coefficient in the new term. This is a new parameter of the problem and is called the re-ignition parameter. The resulting equations are simplified and stochastic differential equations for the scalar dissipation rate and the re-ignition parameter are formulated. The system of equations is solved using Monte Carlo calculations. The results show that the newly appearing transport term acts by modifying the S-shaped curve such that the lower turning point appears at higher scalar dissipation rate. In an *a priori* study, predictions using this model are compared with data from a direct numerical simulation of non-premixed combustion in isotropic turbulence simulating extinction and re-ignition.

1. Introduction

The ability of unsteady laminar flamelet models to yield accurate predictions in non-premixed turbulent reacting flows has been investigated in many different studies. These include different geometries and flow situations, such as jet flames [1, 2], diesel engines [3, 4], and gas-turbines [5]. Results of these studies show that even complex chemical processes, such as the formation of NO_x and soot, can be described with reasonable accuracy.

[3] Author to whom correspondence should be addressed.

A particularly appealing feature of the model is that the local instantaneous scalar dissipation rate appears explicitly as a parameter in the model. It describes the rate of molecular mixing of fuel and oxidizer and is known to be a very important parameter in non-premixed combustion. This permits the study of the influence of this important quantity and simplifies the physical interpretation.

However, because of the simplifications made in the derivation of the flamelet equations, the model is generally not valid for arbitrary situations and fails, for instance, in predicting lifted flames or when local extinction and re-ignition events become important.

Local extinction and re-ignition has recently become one of the most prominent research topics in non-premixed turbulent combustion. Many studies have been devoted to this problem, including laboratory experiments [6], direct numerical simulations (DNS) [7], and modelling studies, including transported probability density function (pdf) methods [8], one-dimensional turbulence modelling [9], and conditional moment closure [10, 18]. The Sandia flame series, investigated experimentally by Barlow and Frank [6], consists of six flames with different Reynolds numbers and degrees of local extinction. These flames have become a benchmark data set for modelling studies.

Xu and Pope [8] have presented predictions of three different Sandia flames, varying from moderate to high degree of local extinction, with reasonable agreement with the experiments. In this study, only the ensemble-averaged value of the scalar dissipation rate is used in the simulations, and fluctuations of this quantity are neglected.

The influence of the fluctuations of the scalar dissipation rate has recently been investigated by Pitsch and Fedotov [11]. In this work, the flamelet equations were used with the scalar dissipation rate as a random variable. To describe the evolution of the scalar dissipation rate, a stochastic differential equation (SDE) was formulated and a Fokker–Planck equation for the joint pdf of the stoichiometric temperature and the scalar dissipation rate was derived. It was shown that the fluctuations of the scalar dissipation rate can lead to local extinction even when the average scalar dissipation rate is below the extinction limit. Moreover, analysis of the equations demonstrates that, when applying the unsteady flamelet equations, re-ignition can only occur if an extinguishing flame particle crosses the so-called S-shaped curve, where a flame particle is characterized by the stoichiometric temperature and dissipation rate. Practically, considering a system at ambient conditions, this can happen only at still very high temperature. Hence, the study presented in [11] essentially neglected re-ignition phenomena, and the real behaviour of a physical system could not be investigated.

In this work, an extension of the flamelet model is presented, which can account for re-ignition. Extinction by locally excessive scalar dissipation rates causes low temperature regions to occur on the surface of the stoichiometric mixture, which will be neighboured by still burning, and therefore, hot regions. We will assume that re-ignition occurs by partially-premixed flame propagation along the surface of the stoichiometric mixture. In flamelet modelling, the transport along this surface is neglected and single flamelets cannot account for re-ignition. Here, the corresponding transport terms are not neglected and, upon modelling, account for the interaction between individual flamelets. The resulting modelled equations are solved numerically and the mechanisms of extinction and re-ignition are investigated.

2. Governing equations

2.1. Interacting flamelet model

To derive the interacting flamelet equations, the equation for the temperature T is considered. The interacting flamelet equations for other reactive scalars can be derived similarly. Since

the model will subsequently be compared to the results of DNSs, we assume constant heat capacity c_p and negligible temporal pressure changes and radiative heat loss. The chemistry is described by a one-step reversible reaction with net reaction rate w. A more general formulation accounting for these effects and complex chemistry is a trivial extension of the following derivation. In addition to the temperature equation, we will use the transport equation for the mixture fraction Z. If the Lewis number of the mixture fraction is assumed to be unity, the equations for mixture fraction $Z = Z(t, x_1, x_2, x_3)$ and temperature $T = T(t, x_1, x_2, x_3)$ can be written as

$$\rho \frac{\partial Z}{\partial t} + \rho \boldsymbol{v} \cdot \nabla Z - \nabla \cdot (\rho D \nabla Z) = 0, \tag{1}$$

$$\rho \frac{\partial T}{\partial t} + \rho \boldsymbol{v} \cdot \nabla T - \nabla \cdot (\rho D \nabla T) - \rho \frac{Q}{c_p} w = 0, \tag{2}$$

where t is the time, x_i are the spatial coordinates, ρ the density, $\boldsymbol{v}$ the velocity vector, D the diffusivity of the mixture fraction, and Q is the heat of reaction.

We now want to derive a flamelet equation, which accounts for a burning state, but also for local extinction and re-ignition processes. The derivation of the flamelet equations as proposed by Peters [12, 13] starts from the non-dimensional temperature equation, written in the (x_1, x_2, x_3)-coordinate system. Since the following analysis is performed only locally, the x_1-coordinate is assumed to be normal and the x_2, x_3-coordinates tangential to the flame surface. The error introduced by this assumption has been analysed by Klimenko [14]. A coordinate transformation of the Crocco type is then performed, such that

$$(t, x_1, x_2, x_3) \longrightarrow (t, Z, Z_2, Z_3), \tag{3}$$

in which the mixture fraction is introduced as a new independent coordinate. This implies that the new coordinate is locally attached to an iso-surface of the mixture fraction, say the stoichiometric mixture fraction Z_{st}, and the new coordinates Z_2, Z_3 lie within this surface. Then, the transformation of the derivatives is given by

$$\frac{\partial}{\partial t} \longrightarrow \frac{\partial}{\partial t} + \frac{\partial Z}{\partial t}\frac{\partial}{\partial Z},$$

$$\nabla \longrightarrow \nabla Z \frac{\partial}{\partial Z} + \nabla_{Z\perp} \qquad \text{with } \nabla_{Z\perp} = \begin{pmatrix} 0 \\ \partial/\partial Z_2 \\ \partial/\partial Z_3 \end{pmatrix}. \tag{4}$$

Introducing this into equation (2) and using equation (1) one obtains for $T = T(t, Z, Z_2, Z_3)$

$$\rho \frac{\partial T}{\partial t} - \frac{\rho\chi}{2}\frac{\partial^2 T}{\partial Z^2} - \rho \frac{Q}{c_p} w + \rho \boldsymbol{v} \cdot \nabla_{Z\perp} T - 2\nabla Z \cdot \frac{\partial}{\partial Z}(\rho D \nabla_{Z\perp} T)$$
$$- \nabla_{Z\perp} \cdot (\rho D \nabla_{Z\perp} T) - \nabla_{Z\perp} T \cdot \nabla Z \frac{\partial}{\partial Z}(\rho D) = 0. \tag{5}$$

Note that in equations (2) and (5), there appear two different derivatives with respect to time, which are associated with two different coordinate systems. In equation (2), $\partial T/\partial t$ is the rate of change of temperature as observed at a fixed point in space (x_1, x_2, x_3), whereas in equation (5), $\partial T/\partial t$ represents the rate of change of the temperature when moving with the iso-surface of the mixture fraction at fixed (Z, Z_2, Z_3).

In a subsequent asymptotic analysis, Peters [12, 13] shows that changes of the reactive scalars within surfaces of constant mixture fraction are small compared to changes in the

direction normal to this surface, and can therefore be neglected. This leads to the flamelet equations consisting of the first three terms in equation (5):

$$\rho\frac{\partial T}{\partial t} - \frac{\rho\chi}{2}\frac{\partial^2 T}{\partial Z^2} - \rho\frac{Q}{c_p}w = 0, \tag{6}$$

where the scalar dissipation rate,

$$\chi \equiv 2D(\nabla Z)^2 \tag{7}$$

appears as a new parameter. This equation has been analysed in DNS of isotropic decaying turbulence with initially non-premixed reactants by Sripakagorn *et al* [7]. It has been shown that equation (6) describes the extinction process very well, but fails to predict re-ignition. At locations where local extinction has occurred, the scaling in equation (5) changes and the arguments leading to equation (6) are no longer true. Terms describing transport along surfaces of constant mixture fraction are then of leading order and therefore have to be considered. After extinction, the maximum flamelet temperature is small, and changes in the direction normal to iso-surfaces of the mixture fraction can be neglected. Here, it will be argued that re-ignition occurs by partially-premixed flame propagation along iso-surfaces of the mixture fraction. Indeed, an analysis of the DNS data used below indicates that this is the dominant mechanism for re-ignition [15]. Then, temperature changes along the surface of a stoichiometric mixture occur across a length scale corresponding to the thickness of a premixed stoichiometric laminar flame, l_F, and an asymptotic analysis similar to that of Peters [12] can be performed also for a re-igniting flamelet. Introducing a small parameter $\varepsilon \equiv l_F\nabla Z$, where ε represents the ratio of length scales of order-unity temperature changes in the direction normal to iso-mixture fraction surfaces and in the direction along iso-mixture fraction surfaces, the coordinates Z_2 and Z_3 can be replaced by stretched coordinates such that $\xi_2 = Z_2/\varepsilon$ and $\xi_3 = Z_3/\varepsilon$. Then

$$\nabla_{Z\perp} = \frac{\nabla_{\xi\perp}}{\varepsilon} \qquad \text{with } \nabla_{\xi\perp} = \begin{pmatrix} 0 \\ \partial/\partial\xi_2 \\ \partial/\partial\xi_3 \end{pmatrix}. \tag{8}$$

Introducing equation (8) into equation (5) and keeping only leading-order terms, the equations describing the re-ignition process are obtained as

$$\rho\frac{\partial T}{\partial t} - \nabla_{Z\perp}\cdot(\rho D\nabla_{Z\perp}T) - \rho\frac{Q}{c_p}w = 0, \tag{9}$$

where the original coordinates Z_2 and Z_3 have been re-introduced. Since no scaling has been assumed for the time and the reaction terms, and it is obvious that these terms are important for re-ignition, these have been retained in the equation.

The leading-order equation valid for both the extinction and the re-ignition processes can now be obtained by combining equations (6) and (9), yielding the interacting flamelet equation as

$$\rho\frac{\partial T}{\partial t} - \frac{\rho\chi}{2}\frac{\partial^2 T}{\partial Z^2} - \nabla_{Z\perp}\cdot(\rho D\nabla_{Z\perp}T) - \rho\frac{Q}{c_p}w = 0. \tag{10}$$

In this equation, the second term describes the flamelet-type diffusive transport, while the third term describes the interaction of different flamelets. The coordinates Z_2 and Z_3 still measure physical space, while Z is the mixture fraction. Note, however, that since Z, Z_2, and Z_3 form an orthogonal coordinate system, the partial derivatives with respect to Z_2 and Z_3 have to be evaluated at constant Z.

2.2. *Modelled interacting flamelet equation*

To apply equation (10) in a numerical simulation, the newly appearing diffusion term has to be modelled. A simple modelling approach is to represent this term by a molecular-mixing model frequently used in transported pdf modelling. Using for instance an interaction by exchange with the mean (IEM) model [16], this term can be represented as

$$\frac{1}{\rho}\nabla_{Z\perp}\cdot(\rho D\nabla_{Z\perp}T) = -\frac{T-\langle T|Z\rangle}{T_{\mathrm{IEM}}}, \tag{11}$$

where $\langle T|Z\rangle$ is the ensemble average of the temperature conditioned on a given value of the mixture fraction, and T_{IEM} is the mixing time. An appropriate definition of the ensemble average has to be chosen for a particular application. Below, the model will be used in a comparison with data from a DNS of non-premixed combustion in isotropic decaying turbulence. For this, the ensemble average corresponds to a spatial average at a given time.

The conditional rather than the unconditional average of the temperature has been used in equation (11), since, as mentioned earlier, the diffusion term modelled in equation (11) describes only mixing at a given mixture fraction. It is well known that the application of IEM as a mixing model for reactive scalars creates problems if mixing occurs between states with different mixture fractions. Then pure fuel could for instance be mixed with pure oxidizer, resulting in a stoichiometric non-reacting mixture at low temperature, which is unphysical in a flamelet-type combustion situation. It is interesting to note that in the current application of the IEM model, which only accounts for mixing along surfaces of constant mixture fraction, this problem does not occur.

The modelled interacting flamelet equation is then given as

$$\frac{\partial T}{\partial t} - \frac{\chi}{2}\frac{\partial^2 T}{\partial Z^2} + \frac{T-\langle T|Z\rangle}{T_{\mathrm{IEM}}} - \frac{Q}{c_p}w = 0. \tag{12}$$

The remaining modelling problem is now to determine the mixing time T_{IEM}. This can be done in different ways. A particularly appealing way is to make the assumption that all changes of the temperature along iso-surfaces of the mixture fraction are caused by changes in the scalar dissipation rate. The strength of this assumption is that it incorporates the fact that extinction is caused by excessive scalar dissipation rate. It has, for instance, also been found by Mastorakos *et al* [17] that the scalar dissipation rate and its fluctuations decisively determine auto-ignition delay times in non-premixed turbulent systems. This demonstrates that the scalar dissipation is also a very important parameter of the re-ignition process in non-premixed turbulent combustion. We will therefore introduce the scalar dissipation rate as a new independent coordinate.

For the following derivation, we will first assume that the local instantaneous scalar dissipation rate can be described as a one-parameter function of the mixture fraction

$$\chi(t, x_1, x_2, x_3) = \chi_{\mathrm{st}}(t, x_1, x_2, x_3)\, f(Z). \tag{13}$$

The exact form of the function $f(Z)$ is not important here, and can for instance be taken to be constant, or from a laminar counterflow configuration [12], an unsteady mixing layer [13], or a semi-infinite mixing layer [1]. This assumption is valid at least within a small region around the reaction zone, which is assumed to be laminar, and has also been corroborated by the DNS data used for a validation of the present model [7]. A detailed discussion of this assumption in the context of these DNS data can be found in Cha *et al* [18]. In [18], a transport equation for $\chi_{\mathrm{st}} = \chi_{\mathrm{st}}(t, x_1, x_2, x_3)$ has been given as

$$\rho\frac{\partial \chi_{\mathrm{st}}}{\partial t} + \rho\boldsymbol{v}\cdot\nabla\chi_{\mathrm{st}} - \nabla\cdot(\rho D\nabla\chi_{\mathrm{st}}) - F = 0, \tag{14}$$

where the source term F is given by

$$F = 2\frac{\rho D}{f(Z)}\frac{\partial f(Z)}{\partial Z}\nabla Z\nabla\chi_{\mathrm{st}} + \frac{1}{2}\rho\chi_{\mathrm{st}}^2\frac{\partial^2 f(Z)}{\partial Z^2} + \frac{G}{f(Z)} \tag{15}$$

and G describes the production of scalar dissipation rate by strain-rate fluctuations and the dissipation by molecular diffusion. The source term F in the χ_{st}-equation will not be described in further detail. Production and dissipation processes described by this term will ultimately be modelled by a stochastic process, and F will disappear from the analysis. Note that equation (14) is not restricted to $Z = Z_{\mathrm{st}}$, since χ_{st} is a field quantity, which is defined at any location in space through the local mixture fraction, the local scalar dissipation rate, and equation (13). Hence, χ_{st} is not the scalar dissipation rate at stoichiometric conditions, but a mixture fraction independent quantity, characterizing the magnitude of the local scalar dissipation rate.

Introducing the coordinate transformation equation (4) into equation (14), the χ_{st}-equation becomes

$$\rho\frac{\partial\chi_{\mathrm{st}}}{\partial t} - \nabla_{Z\perp}\cdot(\rho D\nabla_{Z\perp}\chi_{\mathrm{st}}) - F = 0. \tag{16}$$

With the assumption that temperature changes along iso-mixture fraction surfaces are only caused by scalar dissipation rate changes, an additional coordinate transformation $t, Z, Z_2, Z_3 \longrightarrow t, Z, \chi_{\mathrm{st}}$ can be applied to replace the spatial coordinates Z_2 and Z_3 by the scalar dissipation rate, and an additional transport term in scalar dissipation rate space is obtained. The resulting equation is similar to the doubly-conditional moment closure equations [18], but describes local instantaneous instead of conditionally-averaged quantities.

It follows from equation (13) that χ_{st} is not a function of Z, and therefore

$$\nabla_{Z\perp}\chi_{\mathrm{st}} = \nabla_Z\chi_{\mathrm{st}} \qquad \text{with } \nabla_Z = \begin{pmatrix}\partial/\partial Z\\ \partial/\partial Z_2\\ \partial/\partial Z_3\end{pmatrix} \tag{17}$$

and the transformation of the derivatives is given by

$$\frac{\partial}{\partial t} \longrightarrow \frac{\partial}{\partial t} + \frac{\partial\chi_{\mathrm{st}}}{\partial t}\frac{\partial}{\partial\chi_{\mathrm{st}}}, \qquad \nabla_{Z\perp} \longrightarrow \nabla\chi_{\mathrm{st}}\frac{\partial}{\partial\chi_{\mathrm{st}}}. \tag{18}$$

Introducing the coordinate transformation equation (18) into equation (10) and using equation (16), one obtains the equation for $T = T(t, Z, \chi_{\mathrm{st}})$ as

$$\frac{\partial T}{\partial t} + F\frac{\partial T}{\partial\chi_{\mathrm{st}}} - \frac{\chi}{2}\frac{\partial^2 T}{\partial Z^2} - \frac{\gamma_{\mathrm{st}}}{2}\frac{\partial^2 T}{\partial\chi_{\mathrm{st}}^2} - \frac{Q}{c_p}w = 0, \tag{19}$$

where γ_{st} has been introduced as

$$\gamma_{\mathrm{st}} \equiv 2D(\nabla\chi_{\mathrm{st}})^2. \tag{20}$$

Note here that the scalar dissipation rate in the third term of equation (19) is the local, mixture fraction dependent value, remaining from the second term in equation (10), rather than arising from the coordinate transformation. However, it could also be expressed in terms of χ_{st} as $\chi_{\mathrm{st}} f(Z)$. Equation (19) is generally very similar to the flamelet equations given by Peters [13], but two additional terms appear, a convection term in χ_{st}-space caused mainly by random production and dissipation of the scalar dissipation rate, and a diffusion term in χ_{st}-space with γ_{st} as the diffusion coefficient.

The solution of equation (19) describes the temperature evolution in a coordinate system attached to a point of constant mixture fraction and constant scalar dissipation rate. However, we are interested in the development of a flamelet, which is attached to the stoichiometric

surface at the origin of the coordinate system introduced by equation (18). This is generally not at constant scalar dissipation rate, because χ_{st} is a locally fluctuating quantity. The t, Z, χ_{st}-coordinate system moves relative to this because of the production and dissipation of scalar dissipation rate F given by equation (15). We therefore introduce the concept of a flamelet particle and introduce a corresponding coordinate system. Let $\chi_{st}(t)$ be the position of a flamelet particle in χ_{st}-space. By definition, this particle moves with the net production rate F such that

$$\frac{\partial \chi_{st}}{\partial t} = F(t, Z, \chi_{st}(t)). \tag{21}$$

Then equation (19) can be written as

$$\frac{\partial T}{\partial t} - \frac{\chi(t)}{2}\frac{\partial^2 T}{\partial Z^2} - \frac{\gamma_{st}}{2}\frac{\partial^2 T}{\partial \chi_{st}^2} - \frac{Q}{c_p}w = 0, \tag{22}$$

where the scalar dissipation rate $\chi_{st}(t)$ is now a random parameter determined by the solution of equation (21).

We now introduce the non-dimensional temperature θ defined by

$$\theta = \frac{T - T_{st,u}}{T_{st,b} - T_{st,u}} \qquad \text{with } T_{st,u} = T_2 + (T_1 - T_2)Z_{st}, \tag{23}$$

where $T_{st,b}$ is the stoichiometric adiabatic flame temperature as defined in [11], T_1 and T_2 are the temperatures in the fuel and oxidizer, respectively, and the non-dimensional reaction source term ω, also defined in [11], can, for a one-step irreversible reaction, be written as

$$\omega = \mathrm{Da}\frac{(1-\alpha)\exp(\beta_{ref} - \beta)}{1-\alpha(1-\theta)}\left(\frac{Z}{Z_{st}} - \theta\right)\left(\frac{1-Z}{1-Z_{st}} - \theta\right)\exp\left(-\mathrm{Ze}\frac{1-\theta}{1-\alpha(1-\theta)}\right). \tag{24}$$

Here, Da is the Damköhler number, Ze the Zeldovich number, α the heat release parameter, and $\beta = \mathrm{Ze}/\alpha$. The non-dimensional time and scalar dissipation rate are defined as

$$\tau = \frac{\chi_{st,0}}{a}t \qquad \text{and} \qquad x = \frac{\chi}{\chi_{st,0}}, \tag{25}$$

where $a = \Delta Z Z_{st}(1 - Z_{st})$ and $\chi_{st,0}$ is a reference value, here chosen to be the stoichiometric scalar dissipation rate at steady-state extinction conditions. The choice of ΔZ is arbitrary, since each single term equally depends on a. ΔZ has only been introduced for subsequent use in a simplified analytic model, where it will represent a constant reaction zone thickness.

With these definitions, equation (19) can be written as

$$\frac{\partial \theta}{\partial \tau} - \frac{a x(\tau)}{2}\frac{\partial^2 \theta}{\partial Z^2} - \frac{\Upsilon_{st}(\tau)}{2}\frac{\partial^2 \theta}{\partial x_{st}^2} - \omega(\theta) = 0, \tag{26}$$

where Υ_{st} is a dimensionless number representing the ratio of the timescales of the transport in the direction of χ_{st} and the transport in the direction of Z, and is defined by

$$\Upsilon_{st} = \frac{a\gamma_{st}}{\chi_{st,0}^3}. \tag{27}$$

The transport term in the direction of Z always causes heat losses away from the reaction zone. In contrast to this, if a locally extinguished spot is considered, the transport term in the x_{st}-direction can lead to a gain of heat from hotter surrounding areas. Hence, Υ_{st} characterizes the ability to re-ignite and will therefore be called the re-ignition parameter. For $\Upsilon_{st} = 0$, the flamelet equations as given in [11] are recovered.

Based on the assumption that temperature changes along iso-surfaces of the mixture fraction are caused only by changes in the scalar dissipation rate, we have now derived an equation similar to equation (12). However, the present form of the mixing term along mixture

fraction iso-surfaces in equation (26) appears as a mixing term in the x_{st}-direction rather than in physical coordinates, and hence, allows for a more straightforward physical modelling. If in equation (26) the mixing term is modelled in a manner similar to equation (11), dimensional arguments suggest that the mixing time T_{IEM} can be expressed by χ_{st} and γ_{st}. Here, the re-ignition parameter should remain as a fluctuating quantity, while the ensemble average of the scalar dissipation rate is used. The mixing timescale can then be expressed as

$$T_{\mathrm{IEM}} = C_{\mathrm{IEM}} \frac{\langle \chi_{\mathrm{st}}^2 \rangle}{\gamma_{\mathrm{st}}} = \frac{a}{\chi_{\mathrm{st},0}} \frac{\langle x_{\mathrm{st}}^2 \rangle}{\Upsilon_{\mathrm{st}}}. \tag{28}$$

Introducing the IEM-model for the diffusion term in the x_{st}-direction in equation (26) with the timescale modelled by equation (28), we obtain

$$\frac{\partial \theta}{\partial \tau} - \frac{ax}{2} \frac{\partial^2 \theta}{\partial Z^2} + \frac{\Upsilon_{\mathrm{st}}}{2\langle x_{\mathrm{st}}^2 \rangle} \frac{\theta - \langle \theta | Z, \Upsilon_{\mathrm{st}} \rangle}{C_{\mathrm{IEM}}} - \omega(\theta) = 0, \tag{29}$$

where $\langle \theta | Z, \Upsilon_{\mathrm{st}} \rangle$ is the mean temperature, conditioned on Z and Υ_{st}, of the system at a particular time τ. The constant C_{IEM} will be set to unity for subsequent numerical simulations.

2.3. Stochastic differential equations for x_{st} and Υ_{st}

In equation (29), x_{st} and Υ_{st} are fluctuating random quantities. In order to solve this equation, we need to derive SDEs for both. This can be done according to the procedure outlined in [11], which assumes that the stationary distribution of the respective quantity is log-normal. For Υ_{st}, this follows as a consequence of the central limit theorem. Also from the DNS data used below, this has been found to be approximately the case. The resulting equations are

$$\mathrm{d}x_{\mathrm{st}} = -\frac{x_{\mathrm{st}}}{\delta_x} \ln\left(\frac{x_{\mathrm{st}}}{\langle x_{\mathrm{st}} \rangle}\right) \mathrm{d}\tau + \sigma_x \frac{2}{\sqrt{\delta_x}} x_{\mathrm{st}} \circ \mathrm{d}W(\tau) \tag{30}$$

and

$$\mathrm{d}\Upsilon_{\mathrm{st}} = -\frac{\Upsilon_{\mathrm{st}}}{\delta_\Upsilon} \ln\left(\frac{\Upsilon_{\mathrm{st}}}{\langle \Upsilon_{\mathrm{st}} \rangle}\right) \mathrm{d}\tau + \sigma_\Upsilon \frac{2}{\sqrt{\delta_\Upsilon}} \Upsilon_{\mathrm{st}} \circ \mathrm{d}W(\tau), \tag{31}$$

where W is a Wiener process. The same Wiener process has been chosen in equations (30) and (31) to take the correlation between x_{st} and Υ_{st} into account. The symbol $\circ$ appearing in equations (30) and (31) indicates that these have to be understood as being Stratonovich SDEs. δ_x and δ_Υ represent the non-dimensional characteristic timescale for the pdfs of the respective quantity to reach a steady state. σ_x and σ_Υ are the variance parameters of the stationary log-normal pdf.

Equations (29)–(31) denote a closed system of SDEs, which can be solved numerically to obtain the joint pdf of the temperature, the scalar dissipation rate, and the re-ignition parameter in the form $p(\tau, \theta_{\mathrm{st}}, x_{\mathrm{st}}, \Upsilon_{\mathrm{st}})$.

2.4. Simplified interacting flamelet model

In [11], a Fokker–Planck equation for the joint pdf of temperature and the scalar dissipation rate has been given, and the corresponding system of SDEs for temperature and scalar dissipation rate has been discussed. Here, this formulation has been extended to account for re-ignition, resulting in an additional SDE for the re-ignition parameter Υ_{st}. The solution of equations (29)–(31) is fairly straightforward and the additional SDE does not significantly increase the computational cost. However, since the resulting pdf is three dimensional, the computational requirements for achieving similar statistical convergence are substantially higher. For this reason, we want to investigate a simplified model, where only the mean

re-ignition parameter is considered in equation (29) and the SDE for this quantity does not have to be solved. This model will also be compared to the full model to assess the importance of the Υ_{st}-fluctuations.

Multiplying equation (29) with $p(\Upsilon_{st}) = \delta(\Upsilon_{st} - \langle\Upsilon_{st}\rangle)$ and integrating over Υ_{st} yields

$$\frac{\partial\theta}{\partial\tau} - \frac{ax}{2}\frac{\partial^2\theta}{\partial Z^2} + \frac{\langle\Upsilon_{st}\rangle}{2\langle x_{st}^2\rangle}\frac{\theta - \langle\theta|Z\rangle}{C_{IEM}} - \omega(\theta) = 0. \tag{32}$$

This equation can be solved with equation (30) to obtain the joint pdf of temperature and scalar dissipation rate.

3. Results

In this section, a simplified form of equation (32) is used to analyse the influence of the additional transport term in the equation. Results from numerical simulations of the system of SDEs, equations (29)–(31), are discussed for various values of the re-ignition parameter. Finally, the full model and the simplified model based on equation (32) are applied in an *a priori* study and compared to DNS data.

3.1. Analysis

In order to analyse the influence of the additional transport term arising in the model, the transport term in Z will be modelled as described in [11], where also the necessary assumptions are discussed in detail. The equation can then be formulated at Z_{st} leading to

$$\frac{\partial\theta_{st}}{\partial\tau} + x_{st}\theta_{st} + \frac{\Upsilon_{st}}{2\langle x_{st}^2\rangle}\frac{\theta_{st} - \langle\theta_{st}|\Upsilon_{st}\rangle}{C_{IEM}} - \omega(\theta_{st}) = 0. \tag{33}$$

Assuming that Υ_{st} and x_{st} are constant, the steady-state solutions of equation (33) are easily computed. These solutions are shown in figure 1 for varying Υ_{st}. In the case $\Upsilon_{st} = 0$, the well known S-shaped curve is recovered. For the unsteady case, the temporal change of θ_{st} is always negative in the region to the right of the respective curve, and positive in the region to the left of the curve. Hence, if the scalar dissipation rate is increased beyond the value at the upper turning point, extinction occurs. Re-ignition in this case can occur only if the

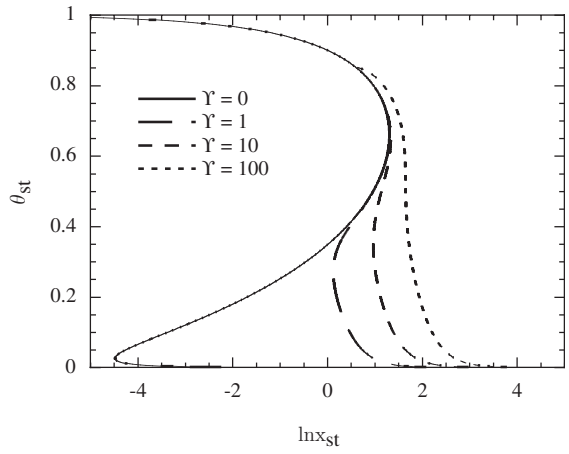

Figure 1. S-curves from steady-state solutions of equation (33) for different values of Υ_{st}.

scalar dissipation rate decreases to values to the left of the S-shaped curve, where the temporal temperature change becomes positive until the upper steady state is reached.

The influence of the diffusion term in χ-space becomes very obvious in the discussion of the steady-state solutions for non-zero $\langle\Upsilon_{st}\rangle$. For $\langle\Upsilon_{st}\rangle = 1$, this transport term leads to a heat flux from the hot surroundings to extinguished particles located on the lower steady branch. This additional term hence leads to a shift of the lower turning point to higher scalar dissipation rates. Extinguished particles can therefore re-ignite at much higher values of the scalar dissipation rate. This trend continues for increasing $\langle\Upsilon_{st}\rangle$. The higher the value of $\langle\Upsilon_{st}\rangle$, the higher the scalar dissipation rate is, which allows for re-ignition. For very large values of $\langle\Upsilon_{st}\rangle$, as shown for $\langle\Upsilon_{st}\rangle = 100$, the turning points of the S-curve, and thereby also extinction as well as re-ignition events, disappear entirely. Then, all states on the steady curve are stable.

3.2. Monte Carlo simulations

In this section, we will first show some results of the model for arbitrarily chosen parameters to further illustrate the influence of the re-ignition parameter in unsteady simulations. Thereafter, we will present an *a priori* validation study of the model using results from a DNS of non-premixed combustion in isotropic decaying turbulence.

3.2.1. Influence of the re-ignition parameter Υ_{st}. For the results presented here, the variance parameters σ and the timescale ratios δ appearing in equations (30) and (31) are all chosen to be unity. For equation (30), this choice has been justified in [11]. All other parameters such as Damköhler number and heat release parameter, have been chosen as in [11]. Three different cases are shown: $\langle\Upsilon_{st}\rangle$ =1, 10, and 100. In addition, the case $\langle\Upsilon_{st}\rangle = 0$ is shown as a reference. This corresponds to the case studied in [11], where the transport in χ-space does not appear in the flamelet equations.

Monte Carlo simulations are used to solve the system of equations (29)–(31). The temperature equation is integrated using a second-order Runge–Kutta scheme. The equations for the SDEs for x_{st} and Υ_{st} are integrated with the second-order accurate method of Milśhtein [19]. Multiple realizations together approximate the joint pdf of θ, χ, and Υ .

Figure 2 shows typical realizations of the system of SDEs. The left-hand figure is for $\langle\Upsilon_{st}\rangle = 0$, the right-hand figure shows particles with the same x_{st}-history, but for $\langle\Upsilon_{st}\rangle = 10$.

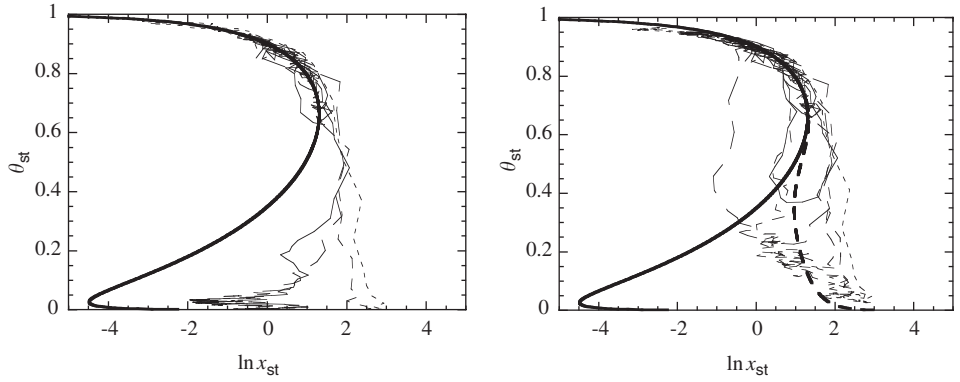

Figure 2. Temporal development of arbitrary extinguishing particles (thin lines) from the solution of equations (29)–(31). Thick lines are steady-state solutions of equation (33) for $\langle\Upsilon_{st}\rangle = 0$ (——) and $\langle\Upsilon_{st}\rangle = 10$ (- - - -).

The figure demonstrates that the interactive model is capable of predicting re-ignition. In both figures the paths of some extinguishing notional particles are shown. As has been discussed earlier, for $\langle \Upsilon_{st} \rangle = 0$, re-ignition cannot occur. This is clearly seen in the left-hand figure. However, for the interactive model in the right-hand figure, re-ignition is observed. During extinction, the particles undergo random changes of the scalar dissipation rate. If, at a given temperature, x_{st} becomes smaller than the corresponding steady solution, the temporal temperature change becomes positive and the particle can re-ignite. This event becomes more likely for non-zero re-ignition parameter, since the associated S-curves move to higher values of the scalar dissipation rate.

The pdfs $p(\theta_{st}, x_{st})$ for $\langle \Upsilon_{st} \rangle = 0, 1, 10$, and 100 are given in figure 3 at the non-dimensional time $\tau = 5$. To present single event solutions of equation (29), here we have to prescribe the conditional mean of the temperature. For all subplots of figure 3, we used the steady-state value corresponding to $x_{st} = 1$ and $\Upsilon_{st} = 0$. Since this value is approximately $\theta_{st} = 0.8$, the Υ_{st}-mixing term leads to heat losses at instantaneous temperatures above this value. For this reason, the pdfs shown in figure 3 depart markedly from the $\langle \Upsilon_{st} \rangle = 0$ solution for high temperatures and high $\langle \Upsilon_{st} \rangle$. For $\langle \Upsilon_{st} \rangle = 0$, a large number of particles is extinguished. Note, however, that this is difficult to observe in the figure, because of the very narrow distribution at low θ_{st}. For $\langle \Upsilon_{st} \rangle = 1$, the scalar dissipation rate where re-ignition can occur is already greatly increased. The pdf has a similar, but more pronounced, S-shape compared with the

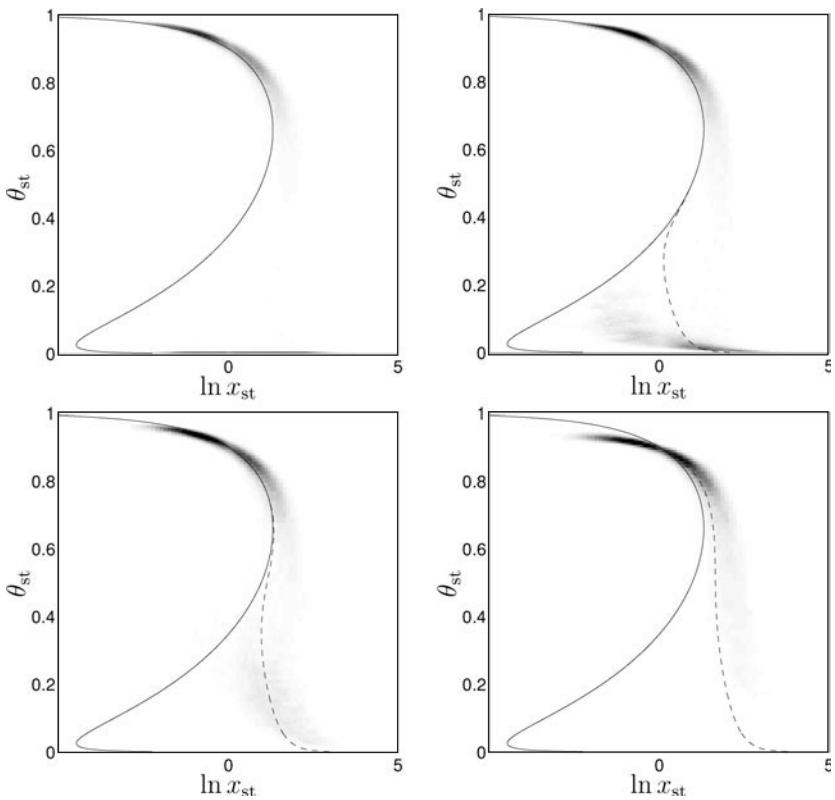

Figure 3. Joint pdfs $p(\theta_{st}, x_{st})$ for $\langle \Upsilon_{st} \rangle = 0$ (upper left), $\langle \Upsilon_{st} \rangle = 1$ (upper right), $\langle \Upsilon_{st} \rangle = 10$ (lower left), $\langle \Upsilon_{st} \rangle = 100$ (lower right); lines are steady-state solutions of equation (33) for the respective $\langle \Upsilon_{st} \rangle$ value (- - - -) and for $\langle \Upsilon_{st} \rangle = 0$ (——).

steady solution curve. On the right-hand side of the steady-state curve, the probability of low temperature is still very high. The reason is that the probability for x_{st} to decrease below the re-ignition value is still very low. At $\langle \Upsilon_{st} \rangle = 10$, the pdf is very similar to the steady-state line, and the probability of low temperatures has strongly decreased. It should be noted that similar S-shaped pdfs have also been found in DNS data [7]. At $\langle \Upsilon_{st} \rangle = 100$, there is no sudden transition from burning to extinguished, since in contrast to the earlier discussed steady-state solutions, the middle branch of the steady-state curve is stable. Hence, there is a relatively low probability of finding low temperatures.

3.2.2. Application to DNS of non-premixed combustion in isotropic turbulence. Further investigation and validation of the proposed model is done by application to the DNS experiment of Sripakagorn *et al* [7]. This DNS has been specifically designed to investigate extinction and re-ignition. A one-step, reversible reaction between fuel and oxidizer evolves in isotropic, homogeneous, and decaying turbulence. Three different simulations, for different frequency coefficients of the global reaction, lead to low, moderate, and high levels of local extinction. These cases are referred to as cases A, B, and C, respectively. For case B, the maximum of the mean stoichiometric scalar dissipation rate is equal to the extinction value of the scalar dissipation rate; for case A, the maximum mean scalar dissipation rate is much lower, and for case C much higher than the extinction value. The numerical parameters used in these simulations are given in [10].

Here, we will present the results of two different models:

(i) The full interacting flamelet model, solving equations (29)–(31). In this model, the temperature θ_{st}, the scalar dissipation rate x_{st} and the re-ignition parameter Υ_{st} are treated as random variables; hence an SDE is solved for each of these quantities.

(ii) The simplified interacting flamelet model, given by the solution of equations (32) and (30). In this model, only the mean of the re-ignition parameter Υ_{st} is considered, and no SDE is solved for Υ_{st}.

All unknown parameters appearing in these equations are taken directly from the DNS data. In particular, figure 4 shows the timescales for the evolution of the pdfs of x_{st} and Υ_{st} from the DNS. As expected, the timescale for the dissipation rate of the dissipation rate is generally much smaller as it is a finer-scale passive quantity. Note that for the present application to

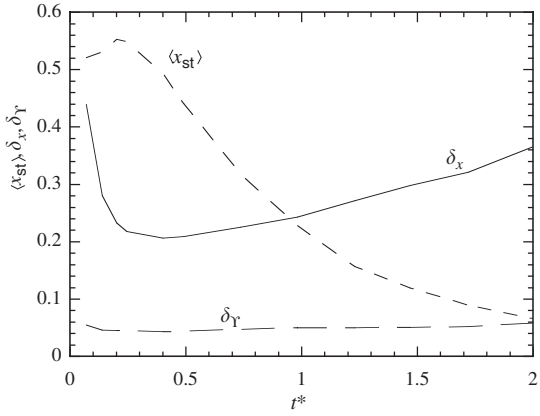

Figure 4. Conditional mean stoichiometric scalar dissipation rate $\langle \chi_{st} \rangle$ and characteristic timescales δ_x and δ_Υ of the pdfs of x_{st} and Υ_{st}.

DNS, the non-dimensionalization from the DNS has been used, which is indicated by referring to t^* instead of τ, which is the time divided by the initial large-eddy turnover time from the DNS. All other non-dimensional quantities are formed accordingly.

The results of the Monte Carlo simulations are compared with DNS data in figure 5. Results are shown from top to bottom in order of increasing level of local extinction. Results of the full model are given in the left-hand column, results of the simplified model in the right-hand

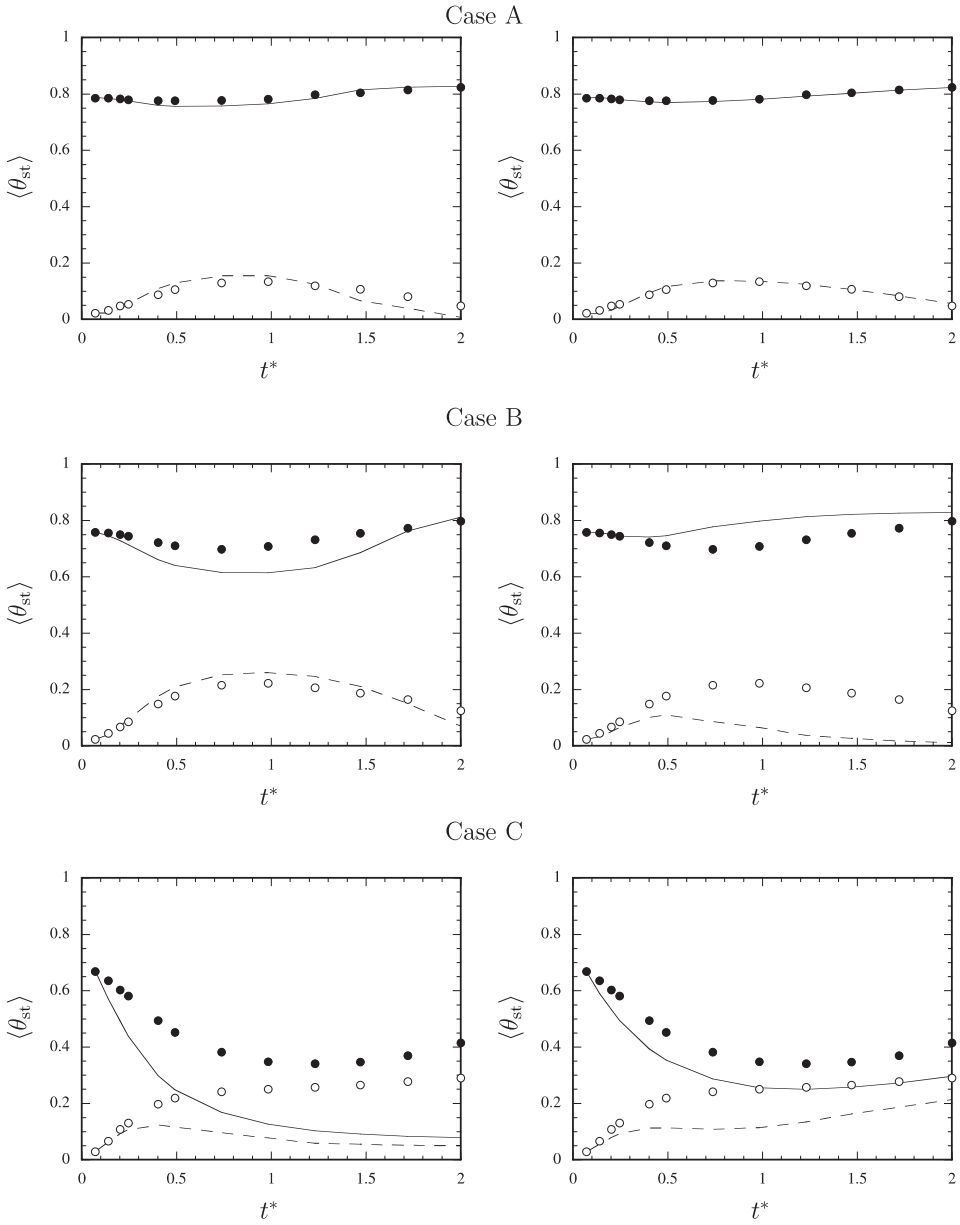

Figure 5. Modelling results (——, - - - -) for the full model (left-hand column) and the simplified model (right-hand column) compared with DNS results (●, ○). Closed symbols are the conditional mean temperature, open symbols the root mean squares.

column. Numerical results are given by the lines, DNS data by the symbols. Closed symbols are the conditional mean temperature, open symbols represent the conditional fluctuations. In the DNS, the mean scalar dissipation rate first increases until approximately $t^* = 0.25$, and decreases afterwards. Correspondingly, all cases show an extinction-dominated phase in the beginning at around $t^* = 0.5$. At later times, when the mean scalar dissipation rate becomes smaller, re-ignition becomes important, and the mean temperature increases again. This is also reflected in the conditional RMS values of the temperature. When the scalar dissipation rate increases, and hence the probability of finding local extinction increases, the pdf of the temperature becomes bimodal and hence the RMS becomes large. During the re-ignition period, extinguished pockets change back to high temperature, the pdf again approaches a unimodal shape, and the RMS values become smaller.

For case A, both models predict the conditional mean as well as the conditional variances very well. For moderate extinction (case B), the full model predicts a consistently lower temperature. The analysis shows that the reason for this is the overprediction of local extinction and is not necessarily related to the re-ignition model. Extinction has been shown in [7] to be well predicted by the unsteady flamelet model if the exact history of the scalar dissipation rate is known. The reason for the present inaccuracies could lie in the fact that the Reynolds number of the DNS might be too low to validate the modelling assumption of a Markovian process for the scalar dissipation rate. This process implies that the rate of change is uncorrelated in time, which will rather be justified at high Reynolds number. The simplified model predicts re-ignition to occur much earlier than the full model does. This also leads to the variance being underpredicted after the onset of the re-ignition process.

For case C, the full model seems to predict extinction of the entire system. This can be seen from the low variance at later times, which indicates that the pdf of temperature becomes unimodal at low temperatures. Note that the present interacting flamelet model has the desirable feature that, if most of the system is extinguished, this model will accelerate extinction of the remaining, still burning parcels, since then, heat losses to extinguished regions become important. However, the underprediction of the temperature is again attributed to the overprediction of extinction at early times. Again, the simplified model predicts the onset of re-ignition much earlier. This leads to the interesting phenomenon that the simplified model correctly predicts re-ignition of the entire system, while the full model does not. However, as in the case of the full model, the amount of local extinction at early times is overpredicted by the simplified model, which seems to compensate for the fact that re-ignition is overestimated.

The uncertainties in the present model can be associated with two main causes: the assumption that the re-ignition process is assumed to be governed by changes in χ only and, second, the errors made in the small-time autocorrelation of χ, which the present stochastic model ignores. Additionally, in the full model, errors can also be impacted by the stochastic modelling of γ as well. Since, for the present cases, we have found that the inaccuracies are given mainly by excessive extinction in the mean, the errors are attributed mainly to the latter reason. The modelling of fluctuations by white noise can be inaccurate, especially for small-scale quantities like χ and γ. In particular, the Markovian assumption is less valid for low Re number, where correlations become stronger. This can cause the model to overpredict the level of extinction for the present DNS. It can therefore be speculated that the application of the present model in a simulation of a realistic case leads to better results.

4. Conclusions

In this work, a model for extinction and re-ignition in non-premixed turbulent combustion based on the flamelet concept is developed. The principal idea is based on the assumptions that

extinction is caused by excessive scalar dissipation rates and that re-ignition occurs by transport of heat and chemical species along mixture fraction iso-surfaces. From these assumptions an interacting flamelet equation can be derived that represents re-ignition by an additional diffusion term. This mixing term accounts for flamelet/flamelet interactions and has been modelled with an IEM approach. The timescale appearing in this model is determined from the assumption that changes along iso-mixture fraction surfaces are caused only by changes of the scalar dissipation rate at this mixture fraction. A newly appearing non-dimensional parameter in the resulting equation describes the ratio of timescales of heat gain along mixture fraction iso-surfaces and diffusive heat losses in the direction normal to these surfaces. This parameter is therefore called the re-ignition parameter.

The model is applied to DNS data of non-premixed combustion in isotropic decaying turbulence with varying degrees of local extinction. The interacting flamelet equation is solved by Monte Carlo simulations with SDEs for the scalar dissipation rate and the re-ignition parameter. To assess the importance of the fluctuations of the re-ignition parameter, a set of simulations is performed using only the conditional average of the re-ignition parameter. In general, the simulations are in reasonable agreement with the DNS data. A possible explanation for the remaining discrepancies could be the inapplicability of the assumptions needed for the derivation of the SDEs for the scalar dissipation rate and the re-ignition parameter for the relatively low Reynolds number of the DNS.

The results show that the dynamics of the interacting flamelet equation are similar to those of the original flamelet equation. The re-ignition parameter modifies the steady-state solutions by increasing the scalar dissipation rate at the lower turning point of the S-shaped curve, thereby allowing re-ignition to the burning state at higher scalar dissipation rates. Interestingly, it is shown that for high values of the re-ignition parameter, the joint pdf of temperature and scalar dissipation rate of the simplified interacting flamelet equations are well described by the steady-state solution of the equation. This could allow the application of simple modelling approaches based only on the steady-state solutions of the interacting flamelet equation for a large re-ignition parameter.

Acknowledgments

The authors gratefully acknowledge funding by the US Department of Energy within the ASCI program and by the Center for Turbulence Research. We also express our gratitude to Paiboon Sripakagorn for making his DNS database available to us before publication.

References

[1] Pitsch H, Chen M and Peters N 1998 Unsteady flamelet modeling of turbulent hydrogen/air diffusion flames *Proc. Combust. Inst.* **27** 1057–64

[2] Pitsch H and Steiner H 2000 Large-eddy simulation of a turbulent piloted methane/air diffusion flame (Sandia flame D) *Phys. Fluids* **12** 2541–54

[3] Pitsch H, Barths H and Peters N 1996 Three-dimensional modeling of NO_x and soot formation in di-diesel engines using detailed chemistry based on the interactive flamelet approach *SAE Paper* 962057

[4] Barths H, Pitsch H and Peters N 1999 3d simulation of di diesel combustion and pollutant formation using a two-component reference fuel *Oil Gas Sci. Technol.-Rev. IFP* **54** 233–44

[5] Barths H, Peters N, Brehm N, Mack A, Pfitzner M and Smiljanovski V 1998 Simulation of pollutant formation in a gas turbine combustor using unsteady flamelets *Proc. Combust. Inst.* **27** 1841–7

[6] Barlow R S and Frank J H 1998 Effect of turbulence on species mass fractions in methane/air jet flames *Proc. Combust. Inst.* **27** 1087–95

[7] Sripakagorn P, Kosály G and Pitsch H 2000 Local extinction–reignition in turbulent nonpremixed combustion *CTR Ann. Res. Briefs* 117–28

[8] Xu J and Pope S B 2000 Pdf calculations of turbulent nonpremixed flames with local extinction *Combust. Flame* **123** 281–307
[9] Hewson J C and Kerstein A R 2001 Stochastic simulation of transport and chemical kinetics in turbulent $CO/H_2/N_2$ flames *Combust. Theory Modelling* **5** 669–97
[10] Cha C M and Pitsch H 2002 Higher-order conditional moment closure modelling of local extinction and reignition in turbulent combustion *Combust. Theory Modelling* **6** 425–37
[11] Pitsch H and Fedotov S 2001 Investigation of scalar dissipation rate fluctuations in non-premixed turbulent combustion using a stochastic approach *Combust. Theory Modelling* **5** 41–57
[12] Peters N 1983 Local quenching due to flame stretch and non-premixed turbulent combustion *Combust. Sci. Technol.* **30** 1–17
[13] Peters N 1984 Laminar diffusion flamelet models in non-premixed turbulent combustion *Prog. Energy Combust. Sci.* **10** 319–39
[14] Klimenko A Y 2001 On the relation between the conditional moment closure and unsteady flamelets *Combust. Theory Modelling* **5** 275–94
[15] Sripakagorn P, Mitarai S, Kosály G and Pitsch H 2002 Extinction and reignition in a diffusion flame (a direct numerical study) *J. Fluid Mech.* submitted
[16] Dopazo C 1975 Probability density function approach for a turbulent axisymmetric heated jet. Centerline evolution *Phys. Fluids* A **18** 397–404
[17] Mastorakos E, DaCruz A P, Baritaud T A and Poinsot T J 1997 A model for the effects of mixing on the autoignition of turbulent flows *Combust. Sci. Tech.* **125** 243
[18] Cha C M, Kosaly G and Pitsch H 2001 Modeling extinction and reignition in turbulent nonpremixed combustion using a doubly-conditional moment closure approach *Phys. Fluids* **13** 3824–34
[19] Milśhtein G N 1978 A method of second-order accuracy integration of stochastic differential equations *Theory Probab. Appl.* **23** 396–401